Journal of Materials Chemistry

Cite this: J. Mater. Chem., 2012, 22, 3916

www.rsc.org/materials

PAPER

Growth of single-crystalline rutile TiO_2 nanorod arrays on GaN light-emitting diodes with enhanced light extraction†

Xiaoyan Liu,[ab] Weijia Zhou,[a] Zhengmao Yin,[a] Xiaopeng Hao,*[a] Yongzhong Wu*[a] and Xiangang Xu[ab]

Received 4th September 2011, Accepted 21st December 2011
DOI: 10.1039/c2jm14369k

TiO_2 is a wide band gap semiconductor with important applications in photovoltaic cells and photocatalysis. In this paper, single-crystalline rutile TiO_2 nanorod arrays were fabricated on the GaN based light emitting diodes (LEDs) with a TiO_2 seed layer by an acid hydrothermal process. The morphologies and the crystallinity of the rutile TiO_2 nanorod arrays on GaN wafer were characterized by scanning electron microscopy, high-resolution transmission electron microscopy and X-ray diffraction. The optical properties of surface-textured TiO_2/GaN were measured and analyzed by photoluminescence. The influence and dependence of the TiO_2 nanorod array with the different densities and diameters on the light output of the fabricated GaN wafers were investigated. The light extraction efficiency of GaN LEDs was enhanced by the single-crystalline rutile TiO_2 nanorod array, which showed an eight-fold increase in photoluminescence intensity compared to the normal planar surface. The mechanisms for the enhanced light output of GaN LEDs by the single-crystalline rutile TiO_2 nanorod arrays were discussed.

Introduction

GaN-based light-emitting diodes (LEDs) have attracted considerable interest in their extensive applications, such as automobile indicators, traffic signals, full-color displays and daily lightings, due to the lower power consumption, longer lifetime and eco-friendly nature. The white-light LEDs are the most promising solid-state lighting method to replace the conventional incandescent and fluorescent lamps. The efficiency of LEDs is influenced by both the internal quantum efficiency and photon extraction efficiency.[1] The internal efficiency of GaN-based LEDs has been remarkably improved by developments in metal organic chemical vapor deposition (MOCVD) processes and device fabrication techniques, which has approached 80–90%.[2] However, the light extraction efficiency of GaN-based LED is still limited due to the total internal reflection (TIR) at the high-refractive-index semiconductor-air interface. Light can only travel from the GaN layer to air within a critical angle of 23.6° due to the large difference in refractive index between the GaN film (n = 2.5) and air (n = 1). Approximately only 26% of the internal light can be extracted from a conventional GaN-based LED chip structure with a planar Ag reflector.[3] Other internal light outside the critical angle are reflected from the interface, reabsorbed, and confined internally, reducing the efficiency. Thus, the achievement of high light extraction efficiency is an important issue to improve the light output power in LEDs. To further improve the light extraction efficiency of GaN LEDs, many efforts had been reported, such as roughened surface,[4,5] photonic crystals,[6] growth on patterned sapphire substrates,[7] graded-refractive-index anti-reflective contacts[8] and surface microstructures.[9–12] To form the microstructures on the surface of GaN with the increased light extraction efficiency, many processes, such as lithography,[13] plasma etching[14] and hydrothermal process,[15] have been widely reported.

In the past two decades, there have been great efforts in synthesizing one-dimensional (1-D) metal oxide nanostructures because of their unique shape-dependent electronic and optical properties.[16–18] Titanium dioxide (TiO_2) semiconductor possesses interesting optical, dielectric, and catalytic properties that result in industrial applications such as optical coating, photocatalysis,[19] photovoltaic materials,[20] gas sensors[21] and Li-ion batteries.[22] Among four polymorphs of TiO_2, anatase, rutile, brookite and TiO_2(B), the rutile phase exhibits an excellent combination of physical properties, including exceptional light scattering efficiency, high refractive index, chemical inertness and photocatalytic properties.[23,24] Microstructures based on TiO_2 nanoarrays were formed on the different substrates by vapor-liquid-solid (VLS) techniques, anodization methods and hydrothermal processes, which are used in many applications such as sensors,[25] photonic crystals,[26] dye-sensitized solar cells (DSSC)[27] and photocatalysis.[28,29] Among these methods, hydrothermal

[a]State Key Laboratory of Crystal Materials, Shandong University, 27 Shandanan Road, Jinan, 250100, P.R. China. E-mail: xphao@sdu.edu.cn; wuyz@sdu.edu.cn
[b]ShanDong Inspur HuaGuang Optoelectronics CO., LTD, 1835 Tianchen Street, High-tech Zone, Jinan, 250101, P.R. China

† Electronic supplementary information (ESI) available: Schematic diagram, EL results, transmission spectrum and synthesis parameters of GaN wafers with a single-crystalline rutile TiO_2 nanorod array were shown in Fig. S1, S2, S3 and S4, respectively. See DOI: 10.1039/c2jm14369k

synthesis is a relatively simple method because of its mild experimental conditions and lower cost; therefore, it is a promising approach to prepare large-scale and well-aligned TiO_2 nanoarrays. ZnO nanowire arrays on GaN with the enhanced light extraction fabricated by hydrothermal and MOCVD processes have been widely reported.[30–33] While a few results about the enhancement of light extraction efficiency using TiO_2 nanostructures formed on the GaN LEDs have been reported,[13,26,34] the growth of single-crystalline rutile TiO_2 nanorods array on GaN LEDs to obtain the enhanced light extraction has been not reported.

In this paper, we propose a flexible process for fabricating the single-crystalline rutile TiO_2 nanorod arrays on the output surface of GaN wafers, which enhances light extraction efficiency from GaN layer. Rutile TiO_2 nanorod nanostructures can be fabricated with controlled nanorods density and narrow size distribution. The morphologies, geometry structure and the crystallinity of the single-crystalline rutile TiO_2 nanorod arrays on the GaN were characterized. The structural dependence and optical properties of the TiO_2 nanorod arrays deposited on the GaN layer were analyzed in detail. The mechanisms of the enhanced light extraction efficiency of GaN LEDs using single-crystalline rutile TiO_2 nanorods array were discussed. Compared to the conventional roughening process, this method has been proven to be flexible, low-cost, with rapid processing for the enhancement of light extraction efficiency of GaN LEDs.

Experimental

Growth of the blue GaN LEDs

The GaN-based LED wafers were grown on polished optical-grade c-face sapphire (0001) substrates by a metal organic chemical vapor deposition (MOCVD) system. Trimethylgallium (TMG), trimethylindium (TMI) and NH_3 were used as the Ga, In and N precursors, respectively. The LED structures consists of a 2 μm thick unintentionally doped GaN layer, a 2 μm thick n-type GaN layer, eight pairs of InGaN/GaN multiple quantum well (MQWs) active layers, and a 0.3 μm thick p-type GaN layer. The active layers consisted of eight pairs each with a 3 nm thick InGaN well layer and a 10 nm thick GaN barrier layer in the InGaN/GaN MQW-LED. Above all, the titanium layer with the thickness of 50 nm was deposited on n-type GaN through magnetron sputtering deposition technology. A rutile TiO_2 seeds layer with a yellow color was obtained by annealing the titanium layer at 550 °C in air for 1 h. Thus, the single-crystalline rutile TiO_2 nanorods arrays were grown on the TiO_2 seeds layer. Schematic diagram of the GaN-based LED wafer with the single-crystalline rutile TiO_2 nanorods array was shown in Fig. S1.†

Growth of TiO_2 nanorods array on n-GaN with a TiO_2 seed layer

In a typical synthesis, 10 mL of deionized water was mixed with 10 mL of concentrated hydrochloric acid (HCl, 38 wt%, Analytically pure, China National Medicines Corporation Ltd.) to reach a total volume of 20 mL in a Teflon-lined stainless steel autoclave (25 mL volume). The mixture was stirred at ambient conditions for 5 min before and after the addition of 0.5 mL of tetrabutyl titanate ($C_{16}H_{36}O_4Ti$, Analytically pure, China National Medicines Corporation Ltd.). One piece of GaN substrate (0.5 cm × 1 cm) was ultrasonically cleaned for 10 min in acetone, ethanol and then in distilled water for 30 min. The substrate was placed at an angle against the wall of the Teflon-liner with the TiO_2 seeds layer facing down. The hydrothermal synthesis was conducted at 160 °C for 2 h. After synthesis, the autoclave was cooled to room temperature. The GaN wafer was taken out, rinsed extensively with deionized water and allowed to dry in ambient air. In some control experiments, ultrasonically cleaned GaN substrate without the TiO_2 seeds layer were used to study the effect of the substrate. The different morphologies and densities of single-crystalline rutile TiO_2 nanorods arrays on GaN were generated by adding the different amounts of tetrabutyl titanate, typically 0.2, 0.5 and 2 mL.

Characterization

The surface morphologies of the single-crystalline rutile TiO_2 nanorod arrays on GaN LEDs were examined by field emission scanning electron microscopy (FESEM, HITACHI S-4800) and high-resolution transmission electron microscopy (HRTEM, JOEL JEM 2100). The chemical composition was investigated *via* energy-dispersive X-ray spectroscopy (EDS). To prepare HRTEM samples, substrates with as-grown nanorods were sonicated at mild power in an ethanol solution, and a drop of this solution was put on the 300 mesh Cu grid. The selected-area electron diffraction (SEAD) pattern was taken on the TEM. X-ray powder diffraction (XRD) pattern of the annealed TiO_2 pattern layer on GaN were recorded on a Bruke D8 Advance powder X-ray diffractometer with Cu-Kα ($\lambda = 0.15406$ nm) from 20° to 80°. The effect of the single-crystalline rutile TiO_2 nanorod arrays on the photon extraction efficiency of GaN LEDs was evaluated by photoluminescence (PL, iHR320, HORIBA Jobin Yvon) with an integrating sphere attachment at the room temperature. Excitation light resource is 4 mW laser with an excitation wavelength of 405 nm.

Result and discussion

The single-crystalline rutile TiO_2 nanorods array was grown on GaN wafers by hydrothermal process at 160 °C for 2 h, which was shown in Fig. 1. The images revealed that the entire surface area of GaN layer was covered totally and continuously with the film consisting of rectangular parallelepiped TiO_2 nanorods (Fig. 1a). It is clearly seen that the top surface of these rods are tetragonal in shape with square top facets (Fig. 1b), the expected growth habit for the tetragonal crystal structure. The side surface is relatively smooth and in tetragonal shape (Fig. 1c). For the almost vertically aligned nanorods, the diameter of the nanorods is about 50 nm with a length of about 1 μm. According to Fig. 1c, the corresponding cross-sectional SEM micrographs of the sample with the TiO_2 nanorods array showed the presence of an up to 50 nm thick residual TiO_2 seeds layer between TiO_2 nanorods array and GaN. To check the function of the TiO_2 seeds layer, we employed a GaN substrate without the TiO_2 seeds layer. As a result, the growth of TiO_2 nanorod arrays on the bare GaN substrate was not successful. This is because there is a big lattice mismatch between rutile TiO_2 (002, $d = 0.148$ nm) and the GaN substrate (002, $d = 0.259$ nm), which is 43.2%. After growing TiO_2 nanorods array on the surface of GaN, the wafer

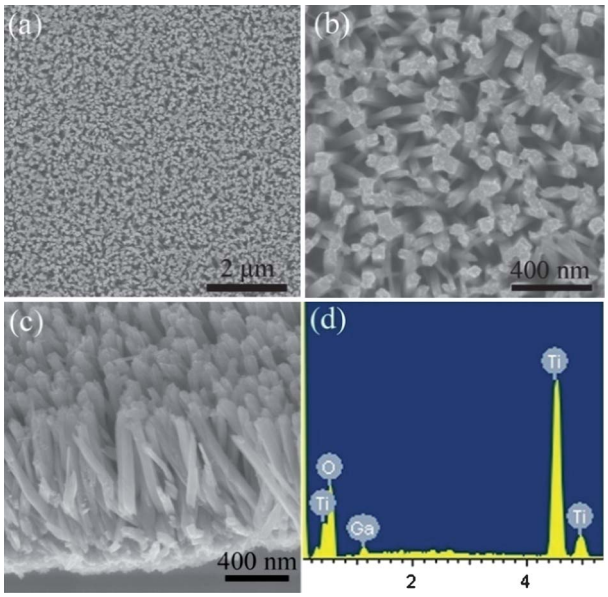

Fig. 1 Typical SEM images with different magnifications (a–c) and EDS result (d) of single-crystalline rutile TiO_2 nanorod arrays on GaN: (a and b) the top view and (c) cross sectional views. For these images, the synthesis process is as follows: hydrothermal treatment at 160 °C for 2 h, 6 M HCl and 0.5 mL tetrabutyl titanate.

still has a good transparence. The transmittance at 465 nm is about 95%, and the corresponding spectrum and images of GaN wafer with TiO_2 nanorod arrays were shown in Fig. S2.† EDX spectrum corresponding to the SEM image detected the composition of the TiO_2 nanorod arrays on GaN wafer (Fig. 1d). Only peaks associated with Ti and O atoms were seen in the EDX spectrum, except for the Ga-related peaks in the spectra that come from the underlying GaN. This revealed that the nanorod array is indeed the TiO_2 material.

Fig. 2 displays the XRD patterns of the GaN wafer before and after the growth of single-crystalline rutile TiO_2 nanorods array by hydrothermal reaction. Before the hydrothermal process, only the strong peak at 34.5° was observed in the curve a, which is due to the (002) face of GaN phase (JCPDS card no. 50-0792, Hexagonal, P63mc, $a = b = 0.319$ nm, $c = 0.518$ nm). After the growth of nanorod arrays on GaN, the peak for GaN was also observed. The other peak at about 62.8° appeared, which was attributed to (002) diffraction peak of rutile TiO_2 (JCPDS card no. 65-0190, Tetragonal, P42/mnm, $a = b = 0.459$ nm, $c = 0.296$ nm). Some rutile diffraction peaks normally presented in polycrystalline powder including (110), (101), (200) and (211) disappeared from the curve b of rutile TiO_2 nanorods array. The results indicated that the as-synthesized array was highly oriented with respect to the substrate surface and the TiO_2 nanorods grown in the [001] direction.[20,27] The results also suggest that the TiO_2 nanorods were not only aligned but are also single-crystalline throughout their length. These conclusions were further confirmed by HRTEM and SAED measurements (Fig. 3).

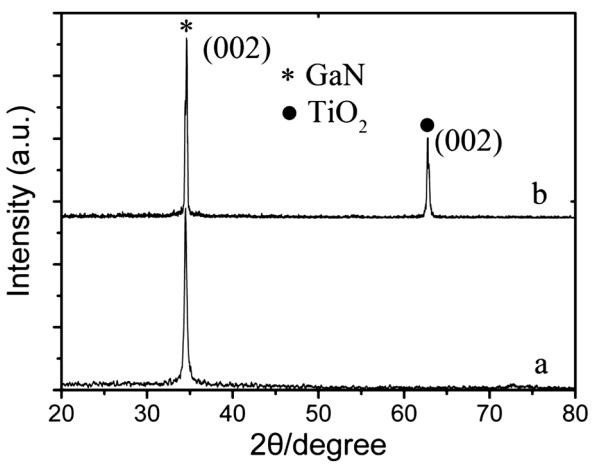

Fig. 2 XRD results of (a) bare GaN and (b) single-crystalline rutile TiO_2 nanorods array on GaN.

The HRTEM images and the selected SAED pattern of a single TiO_2 nanorod were shown in Fig. 3. HRTEM image shows that the typical TiO_2 nanorod exfoliated from the GaN substrate is about 50 nm in diameter and 1 μm in length. The TiO_2 nanorods are completely crystalline along their entire lengths. Lattice images, which are parallel to the long axis, can be clearly seen (Fig. 3a). The distance between the adjacent lattice fringes can be assigned to the interplanar distance of rutile TiO_2 (110) crystal face with the value of 0.32 nm. The [110] axis is perpendicular to the nanorod side walls, and the growth direction along the [001] direction. The SAED pattern (Fig. 3b) also revealed the single-crystalline structure of the nanorod growing along the [001] direction, which was in agreement with the XRD results. The growth habit of crystals is mainly determined by the relative growth of various crystal faces. Depending upon the numbers of corners and edges of the coordination polyhedral available, the growth rate of the different crystal faces of rutile TiO_2 differs and follows the sequence (110) < (100) < (101) < (001).[35] So, growth rate in the [001] direction for rutile TiO_2 is the highest, resulting in the growth of stable c-elongated anisotropic crystals exhibiting (110) faces.[36,37]

The PL emission spectra of the GaN wafers with and without the TiO_2 nanorods array were observed and are shown in Fig. 4a. When 50 nm of a TiO_2 seeds layer was formed on the GaN surface, the intensity of PL emission for the LEDs structure was a little weaker than the reference sample of bare GaN wafer. This behavior was ascribed to the increased back reflection of the inside light from the rutile TiO_2 (n = 2.76)/air interface relative to

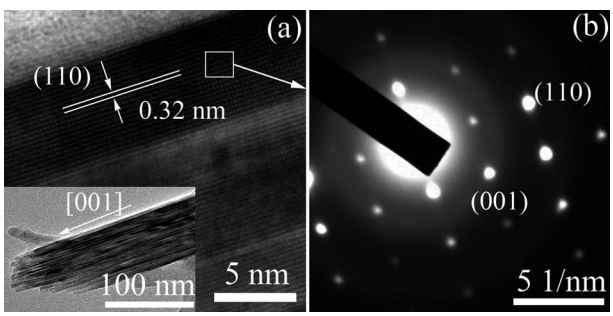

Fig. 3 (a) HRTEM image of a single, single-crystalline rutile TiO_2 nanorod, inset shows the same nanorod and (b) SAED pattern of the same TiO_2 nanorod.

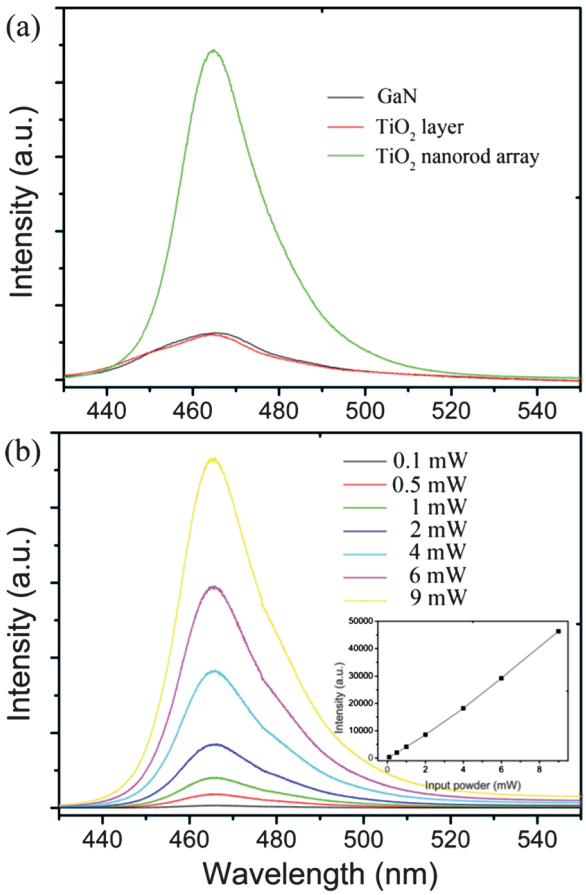

Fig. 4 (a) Comparison of room temperature PL intensity among bare GaN LEDs, GaN LEDs with a TiO_2 seeds layer and GaN LEDs covered with single-crystalline rutile TiO_2 nanorod array. (b) Room temperature PL intensity of TiO_2 nano-patterned GaN LEDs under various input light power (0.1, 0.5, 1, 2, 4, 6 and 9 mW).

the GaN(n = 2.5)/air interface and the increased absorption in the presence of the polycrystalline rutile TiO_2 film.[34] However, the PL intensity of the GaN wafer constructed with single-crystalline rutile TiO_2 nanorods array was much higher, up to eight times stronger than that of the bare GaN wafer. This enhancement can be possibly attributed to the effective refractive index modulation of the GaN layer by the TiO_2 nanorods array and the scatterings of light at TiO_2 nanorods array surface. In the GaN wafer with the rutile TiO_2 nanorods array, the position of the dominated peak located at 465 nm of the PL spectrum was not obviously changed when comparing it with a standard GaN structure that emitted from the GaN MQW active layer. With an increase in the applied input light power from 0.1 to 9 mW, the emission peak intensity of GaN wafer with TiO_2 nanorods array was significantly enhanced without any obvious change of the peak position (Fig. 4b). There was an approximately linear relationship between the PL intensity of GaN wafer with TiO_2 nanorod arrays and input light power (inset in Fig. 4b). Electroluminescence (EL) of GaN wafer with single-crystalline rutile TiO_2 nanorods array was simply tested, which was shown in Fig. S3.† Compared with bare GaN wafer, EL intensity of GaN with TiO_2 nanorods array was remarkably enhanced. At the same time, the illuminated GaN LED wafer with single-crystalline rutile TiO_2 nanorods array at 2 mA was visibly brighter than the reference bare GaN wafer.

The densities and morphologies of the single-crystalline rutile TiO_2 nanorod arrays on GaN could be varied by changing the initial concentration of titanium precursor in the growth solution, which is shown in Fig. 5. It appeared that when the titanium precursor concentration was lower (0.2 mL, Fig. 5a), the TiO_2 nanorods with a lower density were not as aligned as those grown using higher titanium precursor concentrations (0.5 mL, Fig. 1). The nanorods at an angle can keep growing since the probability of running into a neighbour decreases, which induces the polycrystalline TiO_2 layer on GaN. As shown in Fig. 5a, the nanorods grew slightly thinner and shorter with a 20–30 nm diameter and about 0.6 μm in length. The increased amount caused the rapid hydrolysis of tetrabutyl titanate, the continuous TiO_2 film was found to be covered on the GaN layer (Fig. 5b). The continuous film was composed of the TiO_2 nanorods, which were 10 μm in length and 20 nm in diameter (inset in Fig. 5b). XRD results also confirmed the rutile TiO_2 nanorods array with different structures as shown in Fig. 5c. The diffraction peak of GaN was observed in all the rutile TiO_2 nanorods array on GaN substrate. However, the peak intensity for GaN decreased with the increased thickness of the TiO_2 nanorod arrays layer. In the XRD curve of the rutile TiO_2 nanorods array with the low density, the rutile diffraction peaks including (110), (101), (111) and (211) all appeared, suggesting that the rutile TiO_2 nanorods were polycrystalline and not aligned to GaN substrate.[20] While, for the TiO_2 nanorods array and film, only the (002) peak for rutile TiO_2 can be observed (Fig. 5c). PL spectra for the rutile TiO_2 nanorods array grown with different amount of tetrabutyl titanate varying from 0.2, 0.5 to 2 mL were shown in Fig. 5d. Two conditions, a perpendicular array and an appropriate TiO_2 nanorod density, should be satisfied to obtain the highest PL intensity of a single-crystalline rutile TiO_2 nanorod array on

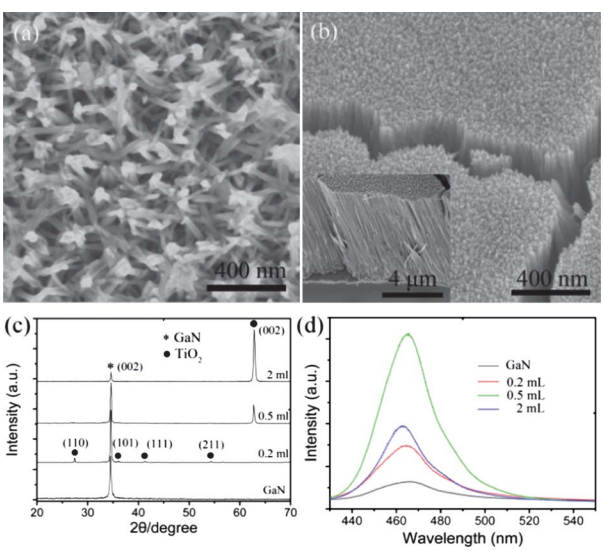

Fig. 5 SEM images of oriented rutile TiO_2 nanorod arrays grown on GaN at 160 °C for 2 h with different amounts of tetrabutyl titanate in a mixture of 20 mL of 6 M hydrochloric acid: (a) 0.2 mL, (b) 2 mL and the corresponding XRD (c) and PL (d) results of GaN covered with rutile TiO_2 nanorod arrays.

GaN. By decreasing the TiO_2 nanorods density on GaN, the light enhancement decreases due to the decrease of TiO_2 nanorods coverage. By increasing the TiO_2 nanorods density on GaN, light absorption increases due to the thicker film. In addition, the effect on the PL intensity of GaN wafers by other experiment parameters, including hydrothermal time and hydrochloric acid concentration are discussed, and are shown in Fig. S4.† Thus, the different rutile TiO_2 nanorods arrays play an important effect on the enhancement of PL intensity of GaN LED wafers.

The mechanisms of the light extraction enhancement by single-crystalline rutile TiO_2 nanorod array on GaN wafers are suggested (Fig. 6). According to Snell's law ($n_1\sin\theta_1 = n_2\sin\theta_2$), the light emitted from the semiconductor into air would be restricted by the total internal reflection effect. The critical angle for the light emission from GaN (n = 2.5) to the air (n = 1) is 23.6°. So, only 4% light in GaN can escape into air (Fig. 6a). After the growth of a rutile TiO_2 seeds layer, numerical simulation indicates that most of the spontaneous emission from the GaN layer will escape into the rutile TiO_2 seed layer due to the higher refractive index of rutile TiO_2 ($n = 2.76$, Fig. 6b).

The combination of surface roughening and the diffraction of the TiO_2 nanorod array, redirect the light into different directions at the interface leading to a larger escape cone to increase the extracted light of GaN over the planar structure of bare GaN (Fig. 6c). The internal light can be all extracted from GaN to the TiO_2 seeds layer according to Snell's law. But, only the light at a larger angle than 68.8° can escape through the TiO_2 nanorods sidewalls. So, no light emission from GaN escaped from the sidewalls of TiO_2 nanorods (curve 1 in Fig. 6c) because all of the light in the TiO_2 seed layer was restricted between 0° and 63.9°. In the diagram, the light emission from the GaN LED can only escape from the rough top of the TiO_2 nanorods. The escape angle is 3° for the light emission along the axial direction of the TiO_2 nanorod and escape from the top, which was depicted as curve (2) in Fig. 6c. The wave-guiding effect of the single-crystalline rutile TiO_2 nanorods as a step index wave-guide optical fiber obtains the increased PL intensity, which was depicted with curve (3) in Fig. 6c. Here, the central TiO_2 nanorods, the core, has a greater refractive index ($n = 2.76$) than the outer region, air

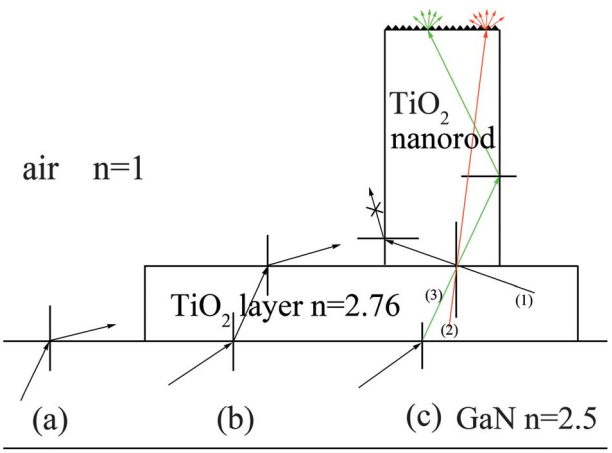

Fig. 6 The schematic view of light escaped from GaN LED covered with single-crystalline rutile TiO_2 nanorod arrays: (a) GaN/air, (b) GaN/TiO_2 layer/air and (c) GaN/TiO_2 layer/TiO_2 nanorod array/air.

($n = 1$). Because of the significant refractive index difference at the TiO_2/air interface, some of the energy from the incident light could be confined within the rod until it escapes at the top end of TiO_2 nanorods.[38] At the same time, the top of TiO_2 nanorods introduce the surface roughness, which is beneficial to the light extraction (Fig. 1b). Light scattering will occur from a random rough surface of the TiO_2 nanorods end, leading to much higher light extraction efficiency. In addition, the rutile TiO_2 nanorods are single-crystalline, which induces a little loss during the light transmission along TiO_2 nanorods. From the above results, we see that the total light extraction efficiency was enhanced by introducing the single-crystalline rutile TiO_2 nanorods array due to the single-crystalline property, wave-guiding effect and rough top surface.

Conclusions

In summary, a highly oriented single-crystalline rutile TiO_2 nanorod array was fabricated on the output surface of the GaN LEDs with a TiO_2 seeds layer using a facile acid hydrothermal process. The diameter of the obtained TiO_2 nanorods was about 50 nm with a length of about 1 μm. The single-crystalline structure of the rutile TiO_2 nanorods grew along the [001] direction, which were aligned to GaN substrate. The growth parameters, like initial Ti^{4+} concentration, could be controlled to fabricate the TiO_2 nanorod arrays with desired densities. The GaN LED with single-crystalline rutile TiO_2 nanorod array patterned surface showed a nearly eightfold increase in the PL intensity compared to the normal planar surface. This improvement in the light extraction efficiency of GaN wafers by the single-crystalline rutile TiO_2 nanorod array were attributed to the increase in the escaping probability of photons from the coarse ends of TiO_2 nanorods and the wave-guiding effect. Single-crystalline rutile TiO_2 nanorod array on GaN locally modulated the refractive index of the GaN layer and enhanced the scattering of light at the interface between GaN and TiO_2. At the same time, single-crystalline rutile TiO_2 nanorods act as wave-guiding media to enhance the light escape from the ends of TiO_2 nanorods. This process provides a low-cost and rapid way to enhance the extraction efficiency of GaN LEDs and modify their output pattern, which has high potential in different fields, such as sensor-arrays, optoelectronic devices, solar cells *etc.* However, experimental conditions need be modified to form the single-crystalline rutile TiO_2 nanorods array onto the complete GaN LED device to obtain a good electroluminescence performance, which requires an in-depth study.

Acknowledgements

This work was financially supported by NSFC (Contract No. 50823009, 51021062), National Basic Research Program of China (2009CB930503), the Fund for the Natural Science of Shandong Province (ZR2010EM020, ZR2010EM049), the Scientific Development Planning of Shandong Province (2010GGX10340), and SRF for ROCS, SEM.

Notes and references

1 K. Okamoto, I. Niki, A. Shvartser, Y. Narukawa, T. Mukai and A. Scherer, *Nat. Mater.*, 2004, **3**, 601–605.

2 T. Nishida, H. Saito and N. Kobayashi, *Appl. Phys. Lett.*, 2001, **79**, 711–712.
3 J. Q. Xi, H. Luo, A. J. Pasquale, J. K. Kim and E. F. Schubert, *IEEE Photonics Technol. Lett.*, 2006, **18**, 2347–2349.
4 T. Fuji, Y. Gao, R. Sharma, E. L. Hu, S. P. DenBaars and S. Nakamura, *Appl. Phys. Lett.*, 2004, **84**, 855–857.
5 J. H. Lee, J. T. Oh, S. B. Choi, Y. C. Kim, H. I. Cho and J. H. Lee, *IEEE Photonics Technol. Lett.*, 2008, **20**, 345–347.
6 W. N. Ng, C. H. Leung, P. T. Lai and H. W. Choi, *Nanotechnology*, 2008, **19**, 255302.
7 R. M. Lin, Y. C. Lu, S. F. Yu, Y. C. S. Wu, C. H. Chiang, W. C. Hsu and S. J. Chang, *J. Electrochem. Soc.*, 2009, **156**, H874–H876.
8 J. K. Kim, S. Chhajed, M. F. Schubert, E. F. Schubert, A. Fischer, M. H. Crawford, J. Cho, H. Kim and C. Sone, *Adv. Mater.*, 2008, **20**, 801–804.
9 H. W. Huang, J. T. Chu, C. C. Kao, T. H. Hseuh, T. C. Lu, H. C. Kuo, S. C. Wang and C. C. Yu, *Nanotechnology*, 2005, **16**, 1844–1848.
10 H. M. Kim, T. W. Kang and K. S. Chung, *Adv. Mater.*, 2003, **15**, 567–569.
11 H. M. Kim, Y. H. Cho, H. Lee, S. I. Kim, S. R. Ryu and D. Y. Kim, *Nano Lett.*, 2004, **4**, 1059–1062.
12 M. K. Lee, C. L. Ho and C. H. Fan, *Appl. Phys. Lett.*, 2008, **92**, 061103.
13 J. Rao, R. Winfield and S. O'Brien, *IEEE Photonics Technol. Lett.*, 2009, **21**, 941–943.
14 T. K. Kim, S. H. Kim, S. S. Yang, J. K. Son, K. H. Lee, Y. G. Hong, K. H. Shim, J. W. Yang, K. Y. Lim, S. J. Bae and G. M. Yang, *Appl. Phys. Lett.*, 2009, **94**, 161107.
15 S. Dalui, C. C. Lin, H. Y. Lee, C. H. Chao and C. T. Lee, *IEEE Photonics Technol. Lett.*, 2010, **22**, 1220–1222.
16 B. Liu and H. C. Zeng, *J. Phys. Chem. B*, 2004, **108**, 5867–5874.
17 R. S. Yang and Z. L. Wang, *J. Am. Chem. Soc.*, 2006, **128**, 1466–1467.
18 D. W. Kim, I. S. Hwang and S. J. Kwon, *Nano Lett.*, 2007, **7**, 3041–3045.
19 W. J. Zhou, H. Liu, J. Y. Wang, D. Liu, G. J. Du and J. J. Cui, *ACS Appl. Mater. Interfaces*, 2010, **2**, 2385–2392.
20 A. Kumar, A. R. Madaria and C. W. Zhou, *J. Phys. Chem. C*, 2010, **114**, 7787–7792.
21 W. J. Zhou, G. J. Du, P. G. Hu, G. H. Li, D. Z. Wang, H. Liu, J. Y. Wang, R. I. Boughton, D. Liu and H. D. Jiang, *J. Mater. Chem.*, 2011, **21**, 7937–7945.
22 G. F. Ortiz, I. Hanzu, P. Lavela, J. L. Tirado, P. Knauthac and T. Djenizian, *J. Mater. Chem.*, 2010, **20**, 4041–4046.
23 D. Wang, D. Choi, Z. Yang, V. V. Viswanathan, Z. Nie, C. Wang, Y. Song, J. Zhang and J. Liu, *Chem. Mater.*, 2008, **20**, 3435–3442.
24 S. Yurdakal, G. Palmisano, V. Loddo, V. Augugliaro and L. Palmisan, *J. Am. Chem. Soc.*, 2008, **130**, 1568–1569.
25 C. L. Cao, C. G. Hua, X. Wang, S. X. Wang, Y. S. Tiana and H. L. Zhang, *Sens. Actuators, B*, 2011, **156**, 114–119.
26 S. K. Kim, H. K. Cho, D. K. Bae, J. S. Lee, H. G. Park and Y. H. Lee, *Appl. Phys. Lett.*, 2008, **92**, 241118.
27 B. Liu and E. S. Aydil, *J. Am. Chem. Soc.*, 2009, **131**, 3985–3990.
28 S. P. Albu, A. Ghicov, J. M. Macak, R. Hahn and P. Schmuki, *Nano Lett.*, 2007, **7**, 1286–1289.
29 D. A. Wang, T. C. Hu, L. T. Hu, B. Yu, Y. Q. Xia, F. Zhou and W. M. Liu, *Adv. Funct. Mater.*, 2009, **19**, 1930–1938.
30 X. M. Zhang, M. Y. Lu, Y. Zhang, L. J. Chen and Z. L. Wang, *Adv. Mater.*, 2009, **21**, 2767–2770.
31 K. K. Kim, S. D. Lee, H. Kim, J. C. Park, S. N. Lee, Y. Park, S. J. Park and S. W. Kim, *Appl. Phys. Lett.*, 2009, **94**, 071118.
32 S. J. An, J. H. Chae, G. C. Yi and G. H. Park, *Appl. Phys. Lett.*, 2008, **92**, 121108.
33 C. B. Soh, C. B. Tay, S. J. Chua, H. Q. Le, N. S. S. Ang and J. H. Teng, *J. Cryst. Growth*, 2010, **312**, 1848–1854.
34 K. M. Yoon, K. Y. Yang, K. J. Byeon and H. Lee, *Solid-State Electron.*, 2010, **54**, 484–487.
35 H. Cheng, J. Ma, Z. Zhao and L. Qi, *Chem. Mater.*, 1995, **7**, 663–671.
36 E. Hosono, S. Fujihara, K. Kakiuchi and H. Imai, *J. Am. Chem. Soc.*, 2004, **126**, 7790–7791.
37 W. J. Zhou, X. Y. Liu, J. J. Cui, D. Liu, J. Li, H. D. Jiang, J. Y. Wang and H. Liu, *CrystEngComm*, 2011, **13**, 4557–4563.
38 K. S. Kim, S. M. Kim, H. Jeong, M. S. Jeong and G. Y. Jung, *Adv. Funct. Mater.*, 2010, **20**, 1076–1082.